Hindawi
Journal of Advanced Transportation
Volume 2022, Article ID 9776845, 18 pages
https://doi.org/10.1155/2022/9776845

*Research Article*

# Energy-Saving Metro Train Timetable Optimization Method Based on a Dynamic Passenger Flow Distribution

**Jingshuang Li**,[1] **Fuquan Pan**,[1] **Hailiang Tang**,[2] **Sen Tong**,[2] **Lixia Zhang**,[1] **Xinguang Li**,[1] **and Xiaoxia Yang**[1]

[1]*School of Mechanical and Automotive Engineering, Qingdao University of Technology, Qingdao 266520, China*
[2]*Qingdao Metro Group Co, Ltd, Qingdao 266045, China*

Correspondence should be addressed to Fuquan Pan; fuquanpan@yeah.net

Received 30 May 2022; Accepted 12 October 2022; Published 22 October 2022

Academic Editor: Yuan Gao



The operation of metro trains with a focus on energy savings can effectively reduce operating costs and carbon emissions. Reducing traction energy consumption and increasing the utilization efficiency of regenerative braking energy are two important energy-saving approaches that are closely related to the metro train interstation running strategy and timetable. Changes in train mass caused by dynamic changes in passenger flow represent one of the important factors affecting the energy consumption and energy-saving operation of metro trains. In this study, the differences in the temporal and spatial distributions of metro line passenger flow were specifically considered, and an energy-saving metro train timetable optimization method focused on the dissipative regenerative braking energy utilization mode was studied. First, a logistic function is used to fit the passenger flow pattern of the origin-destination (OD) station pairs, and the number of passengers getting on and off at each station is derived by establishing the OD dynamic demand matrix for the entire metro line. Then, the passenger load in each station segment is calculated. Next, a timetable optimization model is established to minimize the net energy consumption based on the load difference between station segments and the train motion equation. The interstation running time and dwell time of the metro train are optimized to increase the amount of regenerative braking energy used during the overlap time between the traction and braking actions of adjacent trains in the train operation timetable. A particle swarm optimization and genetic algorithm (PSO-GA) structure is designed to solve the model. The PSO-GA structure has PSO as the main body and integrates the chromosome crossover and mutation operations of the GA into the iterative process to improve the search efficiency of the algorithm. Finally, the proposed method and model are tested based on the actual data of a metro line in Qingdao, China. The goodness of fit of the passenger flow pattern is 0.997. The energy consumption during the study period is reduced by 5169.67 kW h using the optimized timetable. The energy-saving efficiency decreases by 12.18% at a constant OD ratio during the entire travel time and by 20.23% at the same constant load for all station segments. The results of the case analysis prove the effectiveness of the proposed method and model. In addition, the energy-saving timetable can be better optimized by considering the differences in temporal and spatial distributions of dynamic passenger flow.

## 1. Introduction

*1.1. Research Background.* Metro trains feature fast speed, large traffic volume, good punctuality, and high safety standards. They are the backbone of a comprehensive urban transportation system, with vital functions. Compared with ground transportation, metro transportation consumes less energy in transporting the same number of passengers: its energy consumption is 1/3 that of bus transportation and 1/12 that of car transportation (Su et al. [1]). Therefore, metro transportation is considered a green transportation option. However, the energy consumption of the entire metro system is still very high due to its high operating density and long operating mileage. For example, 23 metro lines have been opened and are in operation in Beijing, China, with a total operating mileage of approximately 762 km, and consume more than 50 billion kW·h, which accounts for 1.7% of the total electricity consumption and 14‰ of the

electricity consumption of tertiary industry in China. Research on energy conservation and emission reduction in metro systems is indispensable for reducing operating costs and enhancing environmental protection (Bu et al. [2]).

The energy consumed by the metro system is mainly used for traction power supply, lighting, ventilation and air conditioning systems, escalators, water supply and drainage, and weak current systems. The energy consumption through traction power supply accounts for the largest proportion, namely, 40–50% of the total energy consumption. This is closely related to the operating characteristics of metro trains. Due to the short distance between metro stations and the requirement to provide faster and more efficient transportation services for passengers, metro trains are accelerated quickly and operated at high speeds, so traction power or braking are applied over most of the distance between adjacent stations, which results in high energy consumption. Therefore, reducing the traction power energy consumption is an important and effective energy-saving method for the entire metro system (Su et al. [1]).

Energy-saving train operation control, which is the key to reducing traction energy consumption, is achieved through automatic train operation (ATO), a subsystem of automatic train control (ATC). Specifically, ATO adjusts and converts the four operating modes of traction, cruising, coasting, and braking of a train based on the route parameters, speed limit in each station segment, and real-time train speed, thereby achieving the optimal target speed curve. During train operation, traction energy consumption is mainly related to the magnitude, location, and distance of the traction force, and the speed curve of the train determines the operating modes, the location of each operating mode, and the corresponding distance covered in each operating mode. In other words, multiple sets of speed trajectories are applicable for a train within a certain station segment, and different speed trajectories result in different running time and traction energy consumption between stations (Su et al. [3]). The optimization of the train control strategy can not only effectively reduce the energy consumption during operation and reduce the operation cost but can also greatly improve the comfort, punctuality, and stopping accuracy of train operation (D'Acierno et al. [4]).

In recent years, the popularization of regenerative braking technology has provided a new direction for energy conservation in metro systems (Xin et al. [5]). When a train brakes, the control circuit sends a signal to change the traction motor into reverse work mode, which converts the kinetic energy of the train into electrical energy and feeds the electrical energy back to the catenary, thereby generating regenerative braking energy (Kleftakis et al. [6]). However, if the regenerative braking energy cannot be absorbed synchronously, a voltage surge occurs in the DC catenary, which damages the power system (Kleftakis et al. [6]). From the perspective of the actual operation effect, a certain degree of technical bottleneck is unavoidable in coordinated control with an electrical energy storage device or a power grid, and the regenerative braking energy must be dissipated through resistors if not utilized in a timely manner. Therefore, if the train timetable is adjusted to change the arrival and departure times of trains at each station and the running time of each station segment in the train operation diagram so that a train in the braking mode is adjacent to trains in the traction mode, then the regenerative braking energy can be transferred from the braking train to the traction trains through the catenary to effectively save energy.

Adjusting the operation strategy and running time distribution of a single train in each station segment would also affect the utilization of regenerative braking energy during multitrain operation. Therefore, considering these two aspects is of great significance for comprehensive energy-saving optimization. In recent years, many scholars have carried out relevant studies on the comprehensive optimization of metro train speed trajectories and energy-saving timetables and have made certain achievements (Feng et al. [7]). It is worth noting that the traction force needed by a train is proportional to the total mass of the train, whereas the passenger flow distribution in the metro has temporal and spatial heterogeneity. The constantly changing load factor in different station segments in one day results in changes in the total mass of the train, which affects the energy consumption and the energy-saving efficiency of the system.

To address this problem, in this paper, we first establish an origin-destination (OD) demand time-varying pattern matrix for a metro line from the perspective of cumulative passenger flow demand. In addition, the mathematical models for train operation and timetable-based energy consumption calculation are constructed to optimize the factors in the metro line timetable. Then, the passenger load in each station segment is analyzed and calculated based on the time-varying OD matrix to incorporate the impact of the temporal and spatial distributions of passenger flow on energy consumption in the modelling process to better optimize the energy-saving timetable. In Section 1.2, the current research status of energy conservation in metro systems and some related literature are introduced.

*1.2. Related Literature.* The massive power consumption due to the continuous growth of the metro network has placed great pressure on urban resource carrying capacity. Reducing the energy consumption of the metro system satisfies not only the inherent need to reduce the operating cost but also the external need for sustainable urban development. In general, the energy-saving optimization of metro trains mainly includes two aspects: the optimization of the speed curve of a single train and the optimization of the regenerative braking energy utilization of multiple trains.

The related research on reducing the traction energy consumption of a single train by optimizing the driving control strategy can be traced back to the 1960s. Ichikawa [8] was the first to use the Pontryagin maximum principle to study the energy-saving interstation train operation control problem and proved that maximum traction, cruising, coasting, and maximum braking are the optimal train driving strategies, which have formed the foundation of modern optimal train control theory. Milroy [9] proposed an optimal control model for minimizing the traction energy

consumption of railway trains, with continuously changing traction and braking forces as control variables. Benjamin et al. [10] established a model by setting the operation energy consumption of each operating gear of the train to a fixed unit value and obtained the final solution of the model by finding the operation control sequence with the minimum operation energy consumption. Furthermore, Pudney and Howlett [11] analyzed the energy consumption problem of train operation under the horizontal ramp model and the speed-limited segmented ramp model to determine the transition point of the operating mode sequence with the minimum energy consumption. Howlett [12] minimized the energy consumption of the train by determining the optimal conversion time of the key equation through the Karush–Kuhn–Tucker (KKT) conditions. Hwang [13] optimized the positions of the coasting and braking points of the train by using fuzzy control principles. Khmelnitsky [14] analyzed the energy-saving operation of a train under fixed interstation running time and variable slope and speed limit, but the solution process was complicated. However, limited by the technical conditions at the time, the train control process has been simplified in many ways to construct and solve the models mentioned above.

With the development of computer technology and modern intelligent optimization algorithms, the key technology of train control strategies has been greatly improved, and the study of train speed trajectories has entered a new stage. Chang and Sim [15] constructed a multiobjective model for interstation train running to improve operation energy consumption, punctuality, and ride comfort and obtained the optimal driving strategy through a genetic algorithm (GA). Jin et al. [16] divided the operation section into several representative subsections each containing at most one undulating ramp, optimized the operating mode transition point for any representative subsection according to the operating mode sequence under the given running time conditions, and simulated the relationship between energy consumption and running time through a neural network. Wong and Ho [17] established single-point and multipoint coast control models and searched for the optimal coasting point using a GA to achieve energy-saving train operation. Ke et al. [18] converted the original problem to a problem of optimizing the train speed trajectories on the subsections by dividing the train operation section into several subsections, solved the problem using an ant colony algorithm, and proved that the optimization effect of the algorithm was better than that of the algorithms used in previous studies. Huang et al. [19] solved the proposed model using the particle swarm algorithm to obtain an energy-saving operation strategy for the entire train line. Ahmadi et al. [20] determined the Pareto frontier with the optimal speed and energy consumption through two-stage optimization and then allocated the operating time between stations. In addition, some scholars have noticed such problems in the optimization algorithms as slow convergence and trapping in local optima and have made improvements in related studies. Cao et al. [21] designed a stochastic enhancement algorithm to improve the computational efficiency of speed curve optimization. Liu et al. [22] improved the search method of the control algorithm of the ATO system and experimentally proved the superiority of the improved algorithm-based train operation control over conventional proportional–integral–derivative (PID) algorithm-based train operation control.

Modern metro regenerative braking technology is becoming increasingly mature. The total energy consumption of all trains cannot be minimized through the control strategy of minimizing the energy consumption of a single train, so multi train collaborative energy-saving optimization and train timetable optimization considering the utilization of regenerative braking energy has been drawing increasingly more attention. Andrés et al. [23] optimized the acceleration time and braking time of trains and evaluated the utilization efficiency of the regenerative braking energy of trains by maximizing time synchronization of traction and braking between trains as the objective function. Kim et al. [24] established an integer programming model for train departure time at the departure station to increase the utilization of regenerative braking energy. Nag and Pal [25] established a timetable optimization model considering the utilization of regenerative energy based on the operation of railway trains. Fournier et al. [26] improved the utilization efficiency of regenerative braking energy by optimizing the dwell time of trains and designed a hybrid GA to solve the problem. Hu et al. [27] used particle swarm optimization (PSO) to regulate the train's dwelling time and optimize the trains' schedule, the results of actual optimization examples show that the energy consumption is significantly decreased. Luo et al. [28] established a sparse optimization model by introducing the cardinality function and the square of the Euclidean norm function as the objective function. Li et al. [29] established a nonlinear mixed integer program model, optimized succession time and station dwell act to improve regenerative braking energy utilization rate. Lv et al. [30] analyzed the relationship between the transfer and utilization of regenerative braking energy among trains running in opposite directions and established a mixed integer linear programming model. Liu et al. [31] calculated the energy-saving effect of the timetable for the Batong Metro Line in Beijing in batches using the bacterial foraging optimization strategy and proposed a boundary identification method to measure the traction energy conservation capability of urban rail timetables. Zhang et al. [32] established an overlapping time calculation model to optimize the speed curve, dwell time, and departure interval in the operation scenarios of two trains and three trains, which effectively improved the utilization efficiency of regenerative braking energy. Gao et al. [33] and He et al. [34] obtained an optimal speed curve set of a single train under variable running time based on the Pareto optimal theory and then developed an optimal scheme for allocating the total running time to each station segment through sensitivity analysis.

In recent years, the mathematical models in the relevant literature have been gradually improved. At the same time, many scholars have taken a series of issues related to metro operation into account, making the model closer to reality and more applicable. Jia et al. [35] established a dwell time calculation model based on the analysis of the fluctuation

pattern of boarding and alighting time due to uncertain passenger demands during off-peak hours and allocated the dwell time margin to the interstation running time to reduce energy consumption. Li et al. [36] included the waiting time of incoming and transit passengers as one of the optimization objectives in energy-saving timetable optimization modelling in view of the connection between metro and railway timetables and improved the convenience of transit between different rail transit modes by adjusting the time headway and other factors. Gao et al. [37] and Kang et al. [38] considered the energy-saving problem of trains in skip-stop operation. Although skip-stop operation can better meet the travel needs of passengers and reduce energy consumption, it increases the difficulty of operation and coordination. Qu et al. [39] established an optimization model for minimizing passenger waiting time and total energy consumption considering train delays to enhance the robustness of the energy-saving timetable. Liu et al. [40] took into account the situation that the first and last trains run into operation are both fixed and the travel time duration of each train should be within a predefined window and designed an artificial bee colony (ABC)-based algorithm to solve their model.

Through the analysis of the above documents, many scholars have made a lot of detailed research on the model establishment, algorithm design, and simulation of the optimization of train energy-saving timetable and have made rich research results. However, there are still some shortcomings. In particular, the existing studies often assume that the train load in all station segments is constant, view the dynamic changes in passenger flow from the perspectives of transportation organization and service level (e.g., departure frequency and passenger waiting time), and analyze their effects on timetable formulation without considering the effect of changes in passenger load in each station segment on the calculation of speed curve and energy consumption. Therefore, it is necessary to integrate the spatial-temporal distribution factors of passenger flow into mathematical modelling and to analyze the energy-saving effect to improve theoretical research on the optimization of energy-saving metro train timetables.

*1.3. Main Work.* The main work of this study is as follows:

(1) This study establishes an energy-saving metro timetable optimization model considering factors such as the variation in the actual horizontal and longitudinal sections of the metro line and the regenerative energy utilization relationship between trains running in opposite directions. The simplification of these factors in some previous studies might have reduced the model applicability.

(2) This study characterizes the dynamic pattern of passenger flow based on statistical data to quantitatively reflect the variation in passenger load in each station segment, which provides a basis for model calculation and further improves the relevant theories of energy-saving timetable optimization.

(3) This study verifies the effectiveness of the model and method proposed in this paper through an actual case; the model results under different control variables are comparatively analyzed so that the impact of the dynamic passenger flow distribution on the energy-saving efficiency can be reflected intuitively.

The structure of the rest of this paper is as follows: Section 2 describes the energy-saving train timetable optimization problem considering the dynamic passenger flow distribution. Section 3 constructs mathematical models for the interstation running process, timetable-based energy consumption calculation, and timetable optimization. Section 4 introduces the algorithm design of model solving. Section 5 presents the case analysis. Section 6 shows the discussion in the study. Section 7 is the conclusion.

## 2. Problem Description

*2.1. Speed Curve and Regenerative Braking Energy Utilization.* In general, train operating modes include traction, cruising, coasting, and braking, which correspond to the four stages of the speed curve. If the distance between adjacent stations is small, the cruising stage can be omitted. Taking the train operation process in a certain section as an example, the train departures from station 1 and arrives at station 2. Figure 1 shows the four-stage speed curve and operating mode transition points.

When the train is operating in traction and cruising modes, it needs to obtain electrical energy from the catenary. However, the electrical energy required by the traction mode far exceeds the electrical energy required by the cruising mode. To highlight the research focus, the former is called the energy consumption stage. When the train is operating in braking mode, the electrical energy is generated by regenerative braking technology and fed back to the catenary. This process is referred to as the energy production stage in this paper. The ATC system generates multiple feasible speed trajectories based on the route parameters, train parameters, and interstation running time constraints. Each speed curve has a different interstation running time and operation energy consumption.

The regenerative braking energy utilization of two trains running in the same direction as shown in Figure 2 is used as an example for illustration. When the energy production time window of train 1 overlaps with the energy consumption time window of train 2, the regenerative braking energy generated by train 1 can be utilized by train 2. However, if the transmission distance is too long, the energy loss increases significantly. Therefore, a metro line usually uses multiple power supply zones, and regenerative braking energy generated in one power supply zone cannot be used in another zone. Therefore, although the energy production time window of train 2 overlaps with the energy consumption time window of train 3, the regenerative braking energy cannot be utilized by train 3 since their locations are in different power supply zones. Similarly, the utilization of the regenerative braking energy in trains running the opposite directions can be analyzed.

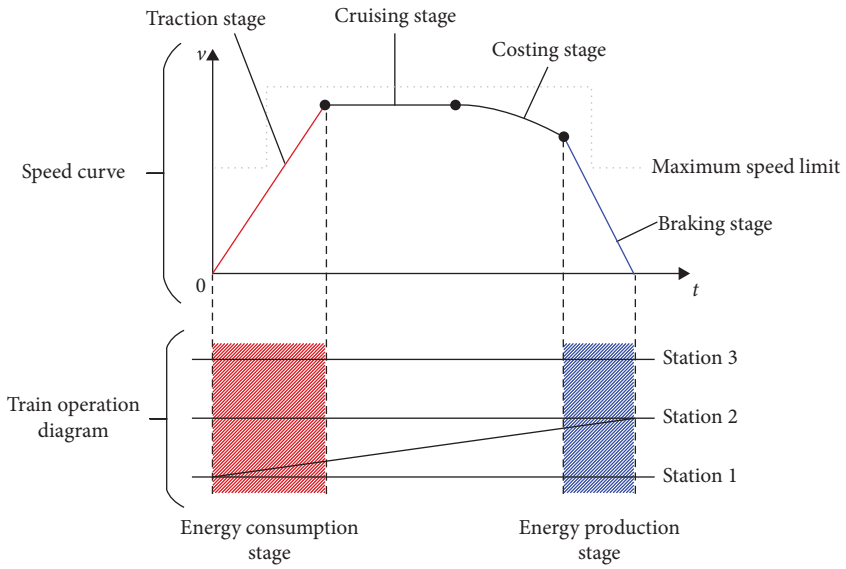


Figure 1: Speed curve of a train running between stations.

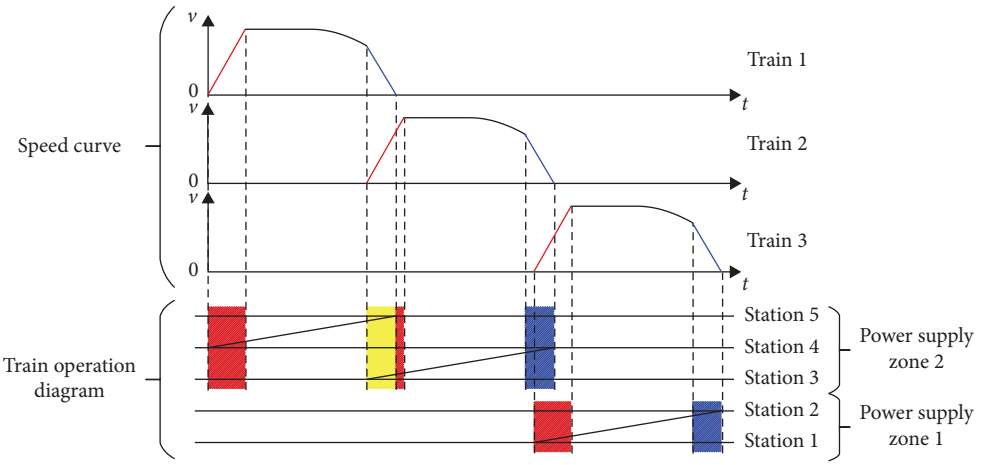


Figure 2: Utilization of regenerative braking energy for two trains running in the same direction.

By extending the utilization of regenerative braking energy from a single train to multiple trains, the elements in the train timetable (such as departure interval, dwell time, and interval running time) can be adjusted and optimized, so that to change the spatiotemporal relationship of multiple train operation in the train diagram, we increase the overlap time of the energy consumption and energy production of different trains in each power supply zone and we make full use of regenerative braking energy as possible. At the same time, based on the analysis and calculation of historical passenger flow statistics, the relationship between the space-time distribution of passenger flow and the optimization of energy-saving schedule can be established, making the optimization effect more realistic.

*2.2. Passenger Load in Each Station Segment.* The passenger flow of the metro exhibits volatility in both the time and space dimensions. The main issue affecting the change in passenger flow over time is that the travel behavior of passengers is different within a day, resulting in dynamic changes in passenger flow over a day with certain regularity. Therefore, the passenger flow density of the same station in each time period is basically the same, and the patterns of the passenger flow changes at different stations are different. The spatial variation in passenger flow is mainly a result of the uneven distribution of passenger flow at each cross section caused by different numbers of boarding and alighting passengers due to the different scales and numbers of passenger entering and leaving at different stations.

To express the characteristics of the dynamic change in passenger flow, the following parameters are defined: $S = \{1, 2, \ldots, 2n\}$. The index is $s$, where $1, 2, \ldots, n$ are the identifiers of upstream stations, and $n+1, n+2 \ldots, 2n$ are the identifiers of downstream stations. Station 1 shares the same platform with station $2n$, station 2 shares the same platform with station $2n-1$;. . .; station $n$ shares the same platform with station $n+1$. $\rho_{s_1,s_2}(t)$ is the passenger flow

density from station $s_1$ to station $s_2$ ($s_1 < s_2$) at the time point $t$. When $s_1 \in \{1, 2, \ldots, n\}$ and $s_2 \in \{n+1, n+2, \ldots, 2n\}$, $\rho_{s_1,s_2}(t) = 0$. $\Pi_{s_1,s_2}(t)$ is the cumulative passenger flow demand from station $s_1$ to station $s_2$ from the time point 0 when the train starts operating to the time point $t$. The relationship between $\Pi_{s_1,s_2}(t)$ and $\rho_{s_1,s_2}(t)$ is expressed as follows:

$$\Pi_{s_1,s_2}(t) = \int_0^t \rho_{s_1,s_2}(t)dt. \tag{1}$$

The cumulative passenger flow demand from station $s_1$ to station $s_2$ within the time window $[t_1, t_2]$ is defined as $\Phi_{s_1,s_2}^{[t_1,t_2]}$. Then, the following equation can be derived from equation (1):

$$\Phi_{s_1,s_2}^{[t_1,t_2]} = \Pi_{s_1,s_2}(t_2) - \Pi_{s_1,s_2}(t_1) = \int_0^{t_2} \rho_{s_1,s_2}(t)dt - \int_0^{t_1} \rho_{s_1,s_2}(t)dt = \int_{t_1}^{t_2} \rho_{s_1,s_2}(t)dt. \tag{2}$$

Within the daily operating time of the metro, the relationship between $\rho_{s_1,s_2}(t)$ and $\Phi_{s_1,s_2}^{[t_1,t_2]}$ and the relationship between $\Pi_{s_1,s_2}(t)$ and $\Phi_{s_1,s_2}^{[t_1,t_2]}$ are shown in Figure 3.

According to Canca et al. [41]and Barrena et al. [42], although the cumulative passenger flow demand curves of different ODs are different, they have a commonality, namely, the presence of several peak demand periods for each OD within the daily operating time, which are caused by the existence of peak passenger flow periods. Therefore, the cumulative passenger flow demand for each OD pair can be represented by $J$ number of linear combinations of S-shaped curves, where $J$ is the number of peak hours, $j$ is the index, and $\Omega_{s_1,s_2}^j$ is the $j$th time period. $\Gamma_{s_1,s_2}^{\text{start}}(j)$ and $\Gamma_{s_1,s_2}^{\text{end}}(j)$ are the starting and ending time points of the time period $\Omega_{s_1,s_2}^j$, respectively. The cumulative passenger flow demand in this period can be obtained by fitting the logistic function, which is expressed as follows:

$$z_{s_1,s_2}(t) = \sum_{j \in J} \left( \frac{K_1^j - K_2^j}{1 + \left(t/t_0^j\right)^r} + K_2^j \right), \tag{3}$$

where $K_1^j$, $K_2^j$, $t_0^j$, and $r$ are the fitting parameters. Equation (3) is solved using the nonlinear least squares method and the values of $J$ and $z_{s_1,s_2}(t)$ to obtain the fitting parameters of the cumulative passenger flow demand curve in each peak period. The value of the logistic function of the passenger flow from station $s_1$ to station $s_2$ in any time period, namely, the passenger flow demand $Z_{s_1,s_2}^{[t_1,t_2]}$, can be calculated by substituting the fitting parameters into equation (3) and considering the distribution of $[t_1, t_2]$:

$$Z_{s_1,s_2}^{[t_1,t_2]} = \begin{cases} \Phi_{s_1,s_2}^{[t_1,t_2]}, & t_1, t_2 \in \Omega_{s_1,s_2}^j \\ \Phi_{s_1,s_2}^{\left[t_1,\Gamma_{s_1,s_2}^{\text{end}}(j)\right]} + \Phi_{s_1,s_2}^{\left[\Gamma_{s_1,s_2}^{\text{start}}(j+1),t_2\right]}, & t_1 \in \Omega_{s_1,s_2}^j, t_2 \in \Omega_{s_1,s_2}^{j+1} \end{cases}. \tag{4}$$

According to the abovementioned method, the time-varying patterns of the cumulative passenger flow for different ODs are fitted, and a dynamic OD demand matrix of the entire metro line is established based on the fitting results:

$$OD(t) = \begin{bmatrix} 0 & z_{1,2}(t) & \cdots & z_{1,2n}(t) \\ z_{2,1}(t) & 0 & \cdots & z_{2,2n}(t) \\ \vdots & \vdots & \ddots & \vdots \\ z_{2n,1}(t) & z_{2n,2}(t) & \cdots & 0 \end{bmatrix}. \tag{5}$$

In the metro system, a large amount of passenger travel data has been collected though the extensively installed automatic fare collection (AFC), and the time-varying pattern of passenger flow between stations can be obtained by mining the ticket and card transaction data provided by the AFC (Yang et al. [43]). Therefore, this paper uses the dynamic OD demand matrix model to characterize the dynamics of passenger demand, which is used as the basis for calculating the passenger load in each station segment in Section 3.1.

## 3. Model Construction

In this section, an energy-saving metro train schedule optimization model is established, and the dynamic distribution of passenger flow on the line are focused, while other actual conditions are also taken into account to enhance the practical value of the model.

*3.1. Assumptions and Notations.* The following assumptions are made to construct the model for the studied problem:

(1) Based on the actual operation conditions, it is assumed that the transportation capacity of the metro line meets the travel demand of passengers with no passenger retention at the platform; that is, all passengers can take the first arriving train to leave after entering the station.

(2) The train timetable is optimized offline; that is, the train operation scheme is determined before departure, and no real-time adjustment is performed after departure. The complete operation process of a train includes the process from the starting station to

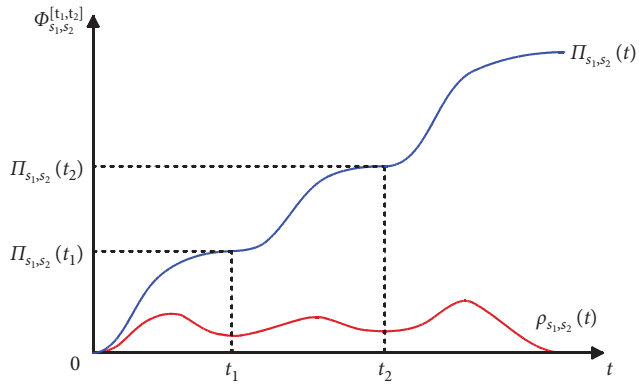


Figure 3: Cumulative passenger flow demand.

the ending station, and the other trains are translated based on departure interval to form a complete train operation diagram.

(3) All trains on the metro line should be the same type with the same number of carriages, and all-stop operation is adopted as the stop mode.

(4) Regenerative braking energy is dissipated, and no energy storage device is installed on the metro line.

Let the interval index be $s'$, $s'$ and $s$ have a one-to-one correspondence, and $s' \neq n, 2n$. The train set is $I$ and the index is $i$. The power supply zone set is $P$ and the index is $p$. The new notations, including symbols, parameters, and decision variables, are shown in Table 1 to describe the proposed mathematical model.

*3.2. Analysis of Interval Passenger Load.* The passenger load of the train in each station segment varies with the passenger flow changes during its operation through the entire metro line, which is expressed as follows:

$$q_{is_\prime} = \begin{cases} b_{is}, & s' = 1, n+1 \\ q_{i(s_\prime-1)} - d_{is} + b_{is}, & otherwise. \end{cases} \tag{6}$$

The number of passengers boarding a train at a certain station is calculated according to equation (5) in Section 2.2, which is expressed as follows:

$$b_{is} = \begin{cases} \sum_{s_0=s+1}^{n} \left[ z_{s,s_0}\left(k_{is}^A\right) - z_{s,s_0}\left(k_{(i-1)s}^D\right) \right], & 1 \le s < n, \\ \sum_{s_0=s+1}^{2n} \left[ z_{s,s_0}\left(k_{is}^A\right) - z_{s,s_0}\left(k_{(i-1)s}^D\right) \right], & n+1 \le s < 2n, \\ 0, & s = n, 2n. \end{cases} \tag{7}$$

Furthermore, the number of passengers alighting from a train when the train arrives at a certain station is the number of passengers with the current station as the destination among all the passengers boarding at the previous stations, i.e.,

$$d_{is} = \begin{cases} \sum_{s_0=1}^{s} b_{is_0}, & 1 < s \le n \\ \sum_{s_0=n+1}^{s} b_{is_0}, & n+1 < s \le 2n \\ 0, & s = 1, n+1 \end{cases}. \tag{8}$$

*3.3. Analysis of Train Operation Process.* The train can be treated as a single mass point when it runs between stations. According to the Newtonian equation, the speed and position of the train running within a station segment at a certain time $t_k$ are expressed as follows:

$$v_{is'}(t_k) = v\left(k_{is}^D\right) + \int_{k_{is}^D}^{t_k} a_{is'}(t)dt \cdot \left(t_k - k_{is}^D\right), t_k \in \left[k_{is}^D, k_{i(s+1)}^A\right], \tag{9}$$

$$l_{is'}(t) = \int_{k_{is}^D}^{t_k} v_{is'}(t_k)dt \cdot \left(t_k - k_{is}^D\right), t_k \in \left[k_{is}^D, k_{i(s+1)}^A\right], \tag{10}$$

When running between stations, the train is affected by gravity and running resistance in addition to the traction and braking forces. The model in this paper considers only the external forces that are in the same plane parallel to the running direction of the train and affect train operation, i.e., traction force, braking force, and running resistance. According to Newton's second law of motion and the

Table 1: Notations of the proposed mathematical model.

| Symbols and parameters | Descriptions |
|---|---|
| $k_{is}^{A}$ | Time when train $i$ arrives at station $s$ |
| $k_{is}^{D}$ | Time when train $i$ departs from station $s$ |
| $\tau_{is'}^{(1)}$, $\tau_{is'}^{(2)}$, $\tau_{is'}^{(3)}$ | Time points when train $i$ transits from traction mode to cruising mode, from cruising mode to coasting mode, and from coasting mode to braking mode in the station segment $s$', respectively |
| $q_{is'}$ | Passenger load of train $i$ during its operation in the interval $s$' |
| $b_{is'}$ | Number of passengers boarding on train $i$ at station $s$ |
| $d_{is'}$ | Number of passengers alighting from train $i$ at station $s$ |
| $F_{is'}^{T}(t)$ | Magnitudes of the traction force on train $i$ when the train is running in the station segment $s$' at time $t$ |
| $F_{is'}^{B}(t)$ | Magnitudes of the braking force on train $i$ when the train is running in the station segment $s$' at time $t$ |
| $f_{is'}(t)$ | Magnitudes of the resistance on train $i$ when the train is running in the station segment $s$' at time $t$ |
| $\widehat{f}_{is'}(t)$ | Unit basic resistance |
| $\widehat{w}_{is'}(t)$ | Unit additional resistance |
| $w_{gre}$, $w_{cre}$, $w_{tre}$ | Additional resistances at the bend, on the ramp, and in the tunnel, respectively |
| $C_1$, $C_2$, $C_3$ | Empirical coefficients |
| $M_{is'}$ | Total mass of train $i$ during its operation in the interval $s$' |
| $M_0$ | No-load mass of the train |
| $\overline{m}$ | Average passenger mass |
| $a_{is'}(t)$ | Acceleration of train $i$ in the station segment $s$' at time $t$ |
| $v_{is'}(t)$ | Speed of train $i$ in the station segment $s$' at time $t$ |
| $l_{is'}(t)$ | Position of train $i$ in station segment $s$' at time $t$ |
| $F_{T,\max}$ | Maximum traction forces |
| $F_{B,\max}$ | Maximum braking forces |
| $\alpha$ | Maximum acceleration |
| $\beta$ | Maximum deceleration |
| $v_{\max}$ | Maximum running speed of the train |
| $L_{is'}$ | Length of station segment $s$' |
| $\Delta t$ | Time granularity |
| $E_{table}^{T}$ | Total traction energy consumption of the timetable |
| $E_{table}$ | Net energy consumption of the timetable |
| $E_{p,\Delta t}^{T}$ | Total amount of traction energy consumed by all trains in the power supply zone $p$ during $\Delta t$ |
| $E_{p,\Delta t}^{B}$ | Total amount of regenerative braking energy produced by all trains in the power supply zone $p$ during $\Delta t$ |
| $\varphi_{is'}$ 0–1 | Binary variable, if the station segment $s$' is located in the power supply zone $p$, then, $\varphi_{is_l} = 1$; otherwise, $\varphi_{is_l} = 0$ |
| $\eta_{me}$, $\eta_{em}$ | Efficiency of conversion from mechanical energy to electrical energy and the efficiency of conversion from electrical energy to mechanical energy, respectively |
| $x_{s',\max}$, $x_{s',\min}$ | Upper and lower limits of the running time in the station segment $s$' |
| $y_{s,\max}$, $y_{s,\min}$ | Upper and lower limits of the dwell time at station $s$ |
| $R_{1,\max}$, $R_{1,\min}$ | Upper and lower limits of the full-line upstream running time, respectively |
| $R_{2,\max}$, $R_{2,\min}$ | Upper and lower limits of the full-line downstream running time, respectively |
| $H_{\max}$, $H_{\min}$ | Maximum and minimum departure intervals, respectively |
| Decision variables | Descriptions |
| $x_{is'}$ | Interstation running time of each train in the station segment $s$' |
| $y_s$ | Dwell time of each train at station $s$ |

descriptions in Section 2.1, the motion equations of the train under the four operating modes when running between stations are as follows:

$$M_{is'}a_{is'}(t) = \begin{cases} F_{is'}^{T}(t) - f_{is'}(t), & t \in \left[k_{is}^{D}, \tau_{is'}^{(1)}\right) \\ 0, & t \in \left[\tau_{is'}^{(1)}, \tau_{is'}^{(2)}\right) \\ -f_{is'}(t), & t \in \left[\tau_{is'}^{(2)}, \tau_{is'}^{(3)}\right) \\ -F_{is'}^{B}(t) - f_{is'}(t), & t \in \left[\tau_{is'}^{(3)}, k_{i(s+1)}^{A}\right] \end{cases}. \quad (11)$$

Because the passenger flow distribution of the metro line has a spatiotemporal heterogeneity, the total mass of the train changes with the variation in its passenger load in each station segment and can be expressed as follows:

$$M_{is'} = M_0 + q_{is'} \cdot \overline{m}. \quad (12)$$

The resistance experienced by trains during operation can be categorized into two types, basic resistance and additional resistance, and their magnitudes are related to the running speed. The basic resistance includes the friction between the various parts of the train, the friction between the wheels and the tracks, and the air resistance. The additional resistance mainly includes the bend resistance, ramp resistance, and tunnel resistance. According to Gao and Yang [44], the resistance on a train can be expressed as follows:

$$\widehat{f}_{is'}(t) = C_1 + C_2 \cdot v_{is'}(t) + C_3 \cdot \left[v_{is'}(t)\right]^2, \tag{13}$$

$$\widehat{w}_{is'}(t) = w_{gre}\left(l_{is'}(t)\right) + w_{cre}\left(l_{is'}(t)\right) + w_{tre}\left(l_{is'}(t)\right), \tag{14}$$

$$f_{is'}(t) = \left[\widehat{f}_{is'}(t) + \widehat{w}(t)\right] \cdot M_{is'}. \tag{15}$$

The energy-saving control strategy of a train in a single station segment prioritizes the use of the maximum traction or braking force. However, when the acceleration exceeds a certain range, passengers feel obvious discomfort and may easily fall or be involved in other accidents. Therefore, the traction and braking forces must be limited to ensure ride comfort. The traction and braking forces on a train running between stations are expressed as follows:

$$F_{i's}^{T}(t) = \begin{cases} \min\left\{F_{T,\max}, M_{is'}\alpha + f_{is'}(t)\right\}, & t \in \left[k_{is}^{D}, \tau_{i's}^{(1)}\right) \\ f_{is'}(t), & t \in \left[\tau_{i's}^{(1)}, \tau_{i's}^{(2)}\right), \\ 0, & \text{otherwise} \end{cases} \tag{16}$$

$$F_{i's}^{B}(t) = \begin{cases} \min\left\{F_{B,\max}, -M_{is'}\beta - f_{is'}(t)\right\}, & t \in \left[\tau_{i's}^{(3)}, k_{i(s+1)}^{A}\right] \\ 0, & \text{otherwise} \end{cases}. \tag{17}$$

The decision variables according to the logical relationship of the train operation diagram can be expressed as follows:

$$x_{s_I} = k_{i(s+1)}^{A} - k_{is}^{D}, \tag{18}$$

$$y_s = k_{is}^{D} - k_{is}^{A}. \tag{19}$$

The train should meet the maximum speed limit during operation, which is expressed as follows:

$$v_{is'}(t) \le v_{\max}. \tag{20}$$

In addition, the train should meet the speed and position limits at the boundary of the interval, which is expressed as follows:

$$v\left(k_{is}^{D}\right) = v\left(k_{i(s+1)}^{A}\right) = 0, \tag{21}$$

$$l\left(k_{i(s+1)}^{A}\right) - l\left(k_{is}^{D}\right) = L_{s'}. \tag{22}$$

### 3.4. Energy-Saving Train Timetable Optimization Model

*3.4.1. Objective Function.* The total traction energy consumption of the timetable is the sum of the energy consumed by each train to overcome the running resistance and to increase the kinetic energy of the train when it is running in each station segment. This is expressed as follows:

$$E_{\text{table}}^{T} = \sum_{i\in I}\sum_{s\in S}\int_{k_{is}^{D}}^{k_{i(s+1)}^{A}} F_{i's}^{T}(t) \cdot v_{is'}(t)dt. \tag{23}$$

The amount of regenerative braking energy utilized is determined by the overlap time of energy consumption and energy production of all trains in the same power supply zone. The time granularity $\Delta t$ is used to calculate the amount of energy consumed and the amount of energy produced, which is expressed as follows:

$$E_{p,\Delta t}^{T} = \sum_{i\in I}\frac{\left[\int_{\Delta t}\varphi_{is'} \cdot F_{i's}^{T}(t) \cdot v_{is'}(t)dt\right]}{\eta_{me}}, \tag{24}$$

$$E_{p,\Delta t}^{B} = \sum_{i\in I}\left[\int_{\Delta t}\varphi_{is'} \cdot F_{i's}^{B}(t) \cdot v_{is'}(t)dt\right] \cdot \eta_{em}. \tag{25}$$

In a metro line without an energy storage device, regenerative braking energy is used immediately after generation, and regenerative braking energy that is not used in time is dissipated in the form of heat energy through resistors. Therefore, the net energy consumption of the timetable is the difference between the total traction energy consumption and the effective utilization of regenerative braking energy, i.e.,

$$E_{\text{table}} = E_{\text{table}}^{T} - \sum_{p\in P}\sum_{\Delta t}\min\left\{E_{p,\Delta t}^{T}, E_{p,\Delta t}^{B}\right\}. \tag{26}$$

By adjusting the train interval operation time and the arrival and departure time of stations along the way, the coordinated optimization of single train operation strategy and the utilization of regenerative braking energy among multiple trains can be realized, so as to achieve the purpose of energy saving of metro system. The optimization objective of the model is to minimize equation (14).

*3.4.2. Constraints.* With the goal of minimizing the net energy consumption of the timetable, the interstation running time of the train and the arrival time at each station are adjusted to achieve the coordinated optimization of the single-train operation strategy and the utilization of regenerative braking energy among multiple trains. The objective function of the timetable optimization model is equation (27).

The constraints of the energy-saving train timetable optimization model are expressed as follows:

$$x_{s',\min} \le x_{s'} \le x_{s',\max}, \tag{27}$$

$$y_{s,\min} \le y_s \le y_{s,\max}, \tag{28}$$

$$R_{1,\min} \le \sum_{s'=1}^{n-1} x_{s'} \le R_{1,\max}, \tag{29}$$

$$R_{2,\min} \le \sum_{s'=n+1}^{2n-1} x_{s'} \le R_{2,\max}, \tag{30}$$

$$H_{\min} \le k^D_{(i+1)s} - k^D_{is} \le H_{\max}. \tag{31}$$

Equation (27) represents the interstation running time constraint. Equation (28) represents the dwell time constraint. Equations (29) and (30) represent the full-line running time constraint. Equation (31) represents the departure interval constraint.

## 4. Algorithm Design

The train timetable optimization problem has a clear application background and is a typical discrete nondeterministic polynomial (NP) problem. An intelligent search is the first choice for solving this type of problem. Intelligent algorithms are particularly effective in solving a train timetable problem that does not consider express service. It should be pointed out that it is important to find a reliable algorithm for the timetable optimization problem. It is of great theoretical and practical significance to design a targeted heuristic algorithm by using the existing solution architecture and combining the characteristics of the problem, or to use the research results of other related disciplines for reference to build a new solution algorithm or architecture.

In this section, a hybrid optimization algorithm based on particle swarm optimization and a genetic algorithm (PSO-GA) is designed, which combines the simple operation and ease of implementation of PSO with the strong global search capabilities and fast convergence of the GA to better solve the model. The solution process is shown in Figure 4.

*4.1. Population Initialization.* The real-number encoded forms of both decision variables are used as the initial positions of the particle: $\Upsilon = \{x_1, x_2, ..., x_{s'}, y_1, y_2, ..., y_s\}$. A total of $N$ feasible particles are randomly generated as the initial population, and the particle index is denoted as $u$. Each particle is randomly assigned an initial speed with the interval $[V_{\min}, V_{\max}]$. The maximum number of iterations is denoted by $G$, and the index of the number of iterations is denoted by $g$.

*4.2. Fitness Function Calculation.* The fitness of each particle $Fit(\Upsilon_u)$ is calculated. The feasibility of $\Upsilon_u$ as a solution is judged. If it is feasible, then, $Fit(\Upsilon_u)$ is calculated by using equation (25) as the fitness function; if it is not feasible, then, $Fit(\Upsilon_u)$ is set to infinity. Let the current particle optimal solution be $o_u$. Then, the optimal solution for the population is $o_N$.

Since the interstation distance of the urban metro lines is generally short, a three-stage (traction, coasting, and braking) speed curve is first calculated. $\tau^{(1)}_{i's}$ and $\tau^{(3)}_{i's}$ are calculated using equations (19-21) and (28). If $v(\tau^{(1)}_{i's}) \le v_{\max}$, then the operating mode transition time of the three-stage speed curve is output. If $v(\tau^{(1)}_{i's}) > v_{\max}$, then $v(\tau^{(1)}_{i's}) = v_{\max}$; at this time, $\tau^{(1)}_{i's}$ has been converted into a known quantity. Next, the cruising stage is introduced into the speed curve, and the speed curve is recalculated with $\tau^{(2)}_{i's}$ as an unknown quantity. Last, the operating mode transition time of the four-stage speed curve is output.

*4.3. Particle Speed and Position Update.* The speed and position of the particles are updated according to the following equations:

$$\begin{aligned} V_u(g+1) = {} & \omega \cdot V_u(g) + \lambda_1 \cdot rand_1 \\ & \cdot (o_u - \Upsilon_u(g)) + \lambda_2 \cdot rand_2 \cdot (o_N - \Upsilon_u(g)), \end{aligned} \tag{32}$$

$$\Upsilon_u(g+1) = \Upsilon_u(g) + V_u(g+1), \tag{33}$$

where $\omega$ is the inertia weight; $\lambda_1$ and $\lambda_2$ are the learning factors; and $rand_1$ and $rand_2$ are random numbers between 0 and 1.

*4.4. Selection, Crossover, and Mutation Operations.* Two different parent particles $u^{(1)}_1$ and $u^{(1)}_2$ are randomly selected. A probabilistic genetic search is performed by simulating binary crossover and polynomial mutation. First, the parameter $\delta$ is determined according to the following equation:

$$\delta = \begin{cases} (2 \cdot ran\ d)^{\frac{1}{1+\varepsilon}}, & ran\ d \le 0.5 \\ 1 - [2(1 - ran\ d)]^{\frac{1}{1+\varepsilon}}, & \text{otherwise} \end{cases}, \tag{34}$$

where $\varepsilon$ is a custom distribution factor. The daughter particles are denoted by $u^{(2)}_1$ and $u^{(2)}_2$, and the simulated binary crossover is expressed as follows:

$$\begin{cases} u^{(2)}_1 = 0.5 \times \left[(1+\delta) \cdot u^{(1)}_1 + (1-\delta) \cdot u^{(1)}_2\right] \\ u^{(2)}_2 = 0.5 \times \left[(1-\delta) \cdot u^{(1)}_1 + (1+\delta) \cdot u^{(1)}_2\right] \end{cases}. \tag{35}$$

The polynomial mutation is expressed as follows:

$$u^{(2)} = u^{(1)} + \delta. \tag{36}$$

*4.5. Termination Decision.* There are two criteria for terminating the algorithm: (1) the number of iterations $g$ reaches the upper limit $G$; (2) the value of the optimal fitness function of the population $o_N$ remains unchanged for $G'$ continuous generations. If any criterion is met, the algorithm is terminated, and the result is output; otherwise, the iteration continues.

## 5. Case Analysis

*5.1. Basic Data.* Based on the relevant data of Qingdao Metro Line 3, a case study was conducted to verify the feasibility and effectiveness of the constructed energy-saving timetable optimization model, and the results were compared with the test results in other scenarios.

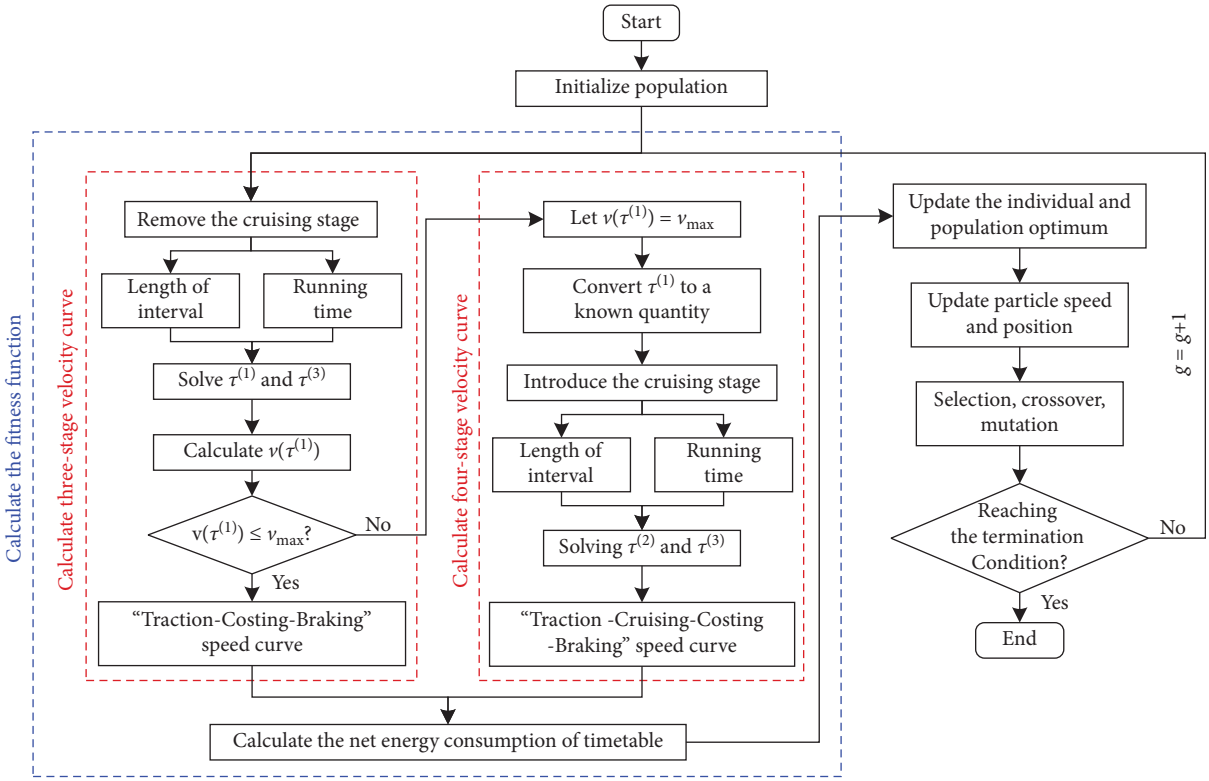


Figure 4: Flowchart of the solution algorithm.

Qingdao Metro Line 3 has a total length of approximately 24.9 km and a total of 22 stations. It uses 6-carriage B-type trains, with a maximum running speed of 80 km/h and running time between 6 : 00 and 23 : 00. The average departure interval is 210 s at the peak periods and 390 s at the nonpeak periods. The interstation running time and dwell time are shown in Table 2. The adjustment range of the interstation running time under the existing scheme shown in Table 2 is set to ±5 s, and the adjustment range of the full-line running time is ±20 s. The energy-saving optimization of the timetable is performed without changing the peak periods or departure intervals of the existing scheme.

According to the information provided by the Qingdao Metro Group Co., Ltd., the parameters in the proposed model are as follows: $M_0 = 192000$ kg; the average passenger mass $\overline{m} = 60$ kg; the empirical coefficients in the unit basic resistance equation $C_1 = 2.031$, $C_2 = 0.062$, $C_3 = 0.001807$; the maximum acceleration $\alpha = 0.8$ m/s$^2$; the maximum deceleration $\beta = -1$ m/s$^2$; the maximum traction and braking forces meet the operational requirements (i.e., the maximum acceleration and maximum deceleration are used in the traction stage and the braking stage, respectively); the efficiency of conversion from mechanical energy to electric energy $\eta_{me} = 0.9$; the efficiency of conversion from electrical energy to mechanical energy $\eta_{em} = 0.85$; and a total of 7 power supply zones are located along the metro line.

The algorithm solution process is performed using MATLAB (version R2021a) on a personal computer equipped with Windows 10 (CPU: i5-10200HQ 2.40 GHz with eight threads, 16.00 GB RAM). The algorithm parameters are set as follows: population size $N = 50$, maximum number of iterations $G = 200$, inertia weight $\omega = 0.9$, learning factors $\lambda_1 = 2.0$ and $\lambda_2 = 2.0$, crossover probability = 0.8, and mutation probability = 0.1.

*5.2. Results and Analysis.* Taking the time period 16 : 00–19 : 00 as an example, the cumulative passenger flow demand from Station 1 to Station 22 in the upstream direction is fitted. This time period contains a complete evening peak $J = 1$. The OD travel data in the AFC system are extracted for fitting, and the fitted curve and the actual data are shown in Figure 5.

Figure 5 shows that the fitted curve basically coincides with the curve of the actual data. The fitting parameters are $K_1^j = 37.44$, $K_2^j = 1499.73$, $t_0^j = 103.97$, and $r = 4.52$. The goodness of fit is 0.997. Therefore, the use of the logistic function to fit the cumulative passenger flow demand has a high reliability. The passenger flow demand in other station segments is similar to that of this station.

Taking the station segment 1 as an example, the variation patterns of traction energy consumption with train mass and running time are obtained by calculating the speed curve under the premise of changing only the train mass and interstation running time without changing other conditions, as shown in Figure 6.

Figure 6 shows that the traction energy consumption increases with increasing train mass and decreases with increasing running time. When the running time increases

Table 2: Interstation running time and dwell time.

| Station name | Up direction number | Interval running time, s | Dwell time, s | Down direction number | Interval running time, s | Dwell time, s |
|---|---|---|---|---|---|---|
| Qingdao Railway Station | 1 | 104 | — | 44 | 104 | — |
| Hall of the PEOPLE | 2 | 96 | 40 | 43 | 96 | 40 |
| Huiquan Square | 3 | 78 | 30 | 42 | 78 | 30 |
| Zhongshan Park | 4 | 84 | 30 | 41 | 84 | 30 |
| Taipingjiao Park | 5 | 107 | 30 | 40 | 107 | 30 |
| Yan'an 3rd Road | 6 | 70 | 45 | 39 | 70 | 45 |
| May 4th Square | 7 | 113 | 45 | 38 | 113 | 45 |
| Jiangxi Road | 8 | 78 | 40 | 37 | 78 | 40 |
| Ningxia Road | 9 | 71 | 35 | 36 | 71 | 35 |
| Dunhua Road | 10 | 74 | 45 | 35 | 74 | 45 |
| Cuobuling | 11 | 105 | 45 | 34 | 105 | 45 |
| Qingjiang Road | 12 | 95 | 40 | 33 | 95 | 40 |
| Shuangshan | 13 | 75 | 45 | 32 | 75 | 45 |
| Changsha Road | 14 | 111 | 30 | 31 | 111 | 30 |
| Metro Building | 15 | 84 | 35 | 30 | 84 | 35 |
| Hai'er Road | 16 | 103 | 30 | 29 | 103 | 30 |
| Wannianquan Road | 17 | 91 | 35 | 28 | 91 | 35 |
| Licun | 18 | 86 | 45 | 27 | 86 | 45 |
| Junfeng Road | 19 | 80 | 35 | 26 | 80 | 35 |
| Zhenhua Road | 20 | 93 | 35 | 25 | 93 | 35 |
| Yongping Road | 21 | 110 | 40 | 24 | 110 | 40 |
| Qingdao North Railway Station | 22 | — | — | 23 | — | — |
| Total | | 1908 | | | 1908 | |

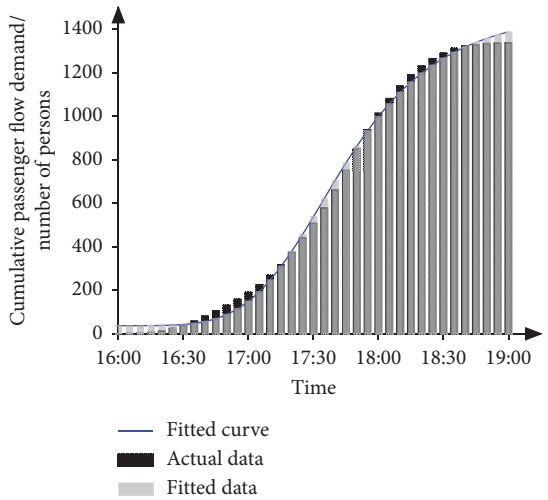


Figure 5: The fitted curve and actual data of the cumulative passenger flow demand.

from 104 s to 114 s, the traction energy consumption decreases by 3.02 kW h (21.45%) and 4.59 kW h (23.03%) when the train masses are 192 t and 292 t, respectively, which indicates that when the train mass is different, the energy-saving potential varies under different running times. Therefore, the differences in the temporal and spatial distributions of the passenger flow along the metro line must be considered to optimize the energy-saving metro train timetable.

The time period 16 : 00–19 : 00 is selected as the study period, and the departure time of all trains in this period is shown in Table 3. There are a total of 41 departures in the upstream direction and 43 departures in the downstream direction. The net energy consumption of the timetable is 25092.64 kW·h. The following four scenarios are set: in Scenario 1, calculations are performed using the parameters provided in the previous section. In Scenario 2, a 6-carriage A-type train is used, and $M_0$ = 222000 kg. In Scenario 3, the difference in the time distribution of passenger flow is not considered, and the passenger load in each station segment is calculated by dividing the cross section passenger flow calculated according to the cumulative OD demand in this period by the total departure frequency of the above-mentioned downlink trains to calculate the average

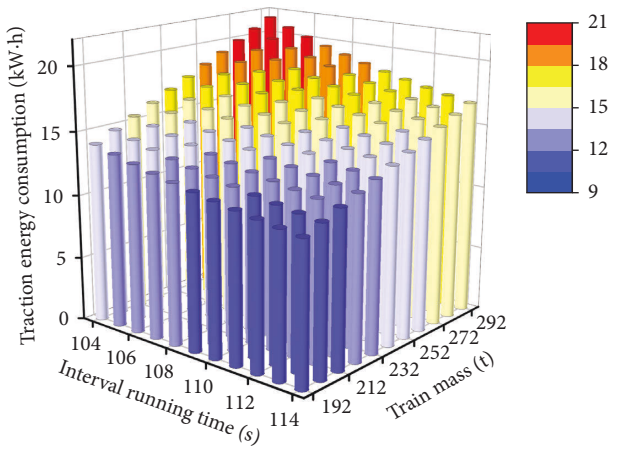


Figure 6: Traction energy consumption in the station segment 1 under different interstation running times and train masses.

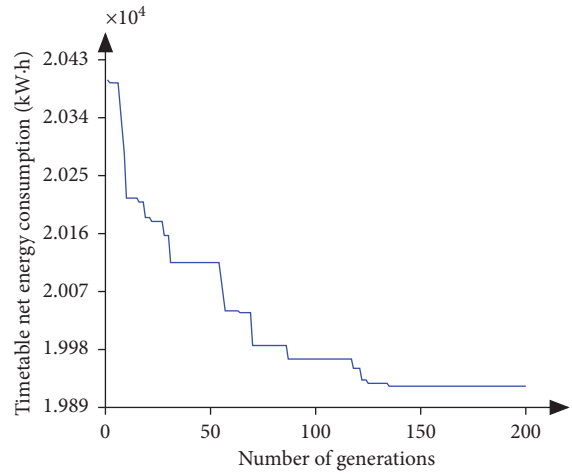


Figure 7: Iterative process finding the optimal total energy consumption value of the timetable.

Table 3: Departure timetable for the time period 16 : 00–19 : 00.

| Up direction departure station: Qingdao Railway Station | | | Down direction departure station: Qingdao North Railway Station | | |
|---|---|---|---|---|---|
| 16 : 04 | 17 : 03 | 18 : 01 | 16 : 02 | 17 : 01 | 18 : 00 |
| 16 : 10 | 17 : 07 | 18 : 05 | 16 : 06 | 17 : 05 | 18 : 04 |
| 16 : 17 | 17 : 11 | 18 : 09 | 16 : 11 | 17 : 09 | 18 : 08 |
| 16 : 23 | 17 : 15 | 18 : 13 | 16 : 15 | 17 : 13 | 18 : 12 |
| 16 : 30 | 17 : 19 | 18 : 17 | 16 : 18 | 17 : 17 | 18 : 16 |
| 16 : 36 | 17 : 22 | 18 : 21 | 16 : 22 | 17 : 21 | 18 : 19 |
| 16 : 43 | 17 : 21 | 18 : 25 | 16 : 26 | 17 : 25 | 18 : 22 |
| 16 : 47 | 17 : 30 | 18 : 29 | 16 : 30 | 17 : 29 | 18 : 27 |
| 16 : 51 | 17 : 34 | 18 : 33 | 16 : 34 | 17 : 33 | 18 : 31 |
| 16 : 55 | 17 : 38 | 18 : 37 | 16 : 38 | 17 : 36 | 18 : 34 |
| 16 : 59 | 17 : 42 | 18 : 40 | 16 : 42 | 17 : 40 | 18 : 41 |
| | 17 : 46 | 18 : 44 | 16 : 46 | 17 : 44 | 18 : 47 |
| | 17 : 50 | 18 : 48 | 16 : 50 | 17 : 48 | 18 : 54 |
| | 17 : 54 | 18 : 52 | 16 : 54 | 17 : 52 | |
| | 17 : 58 | 18 : 56 | 16 : 57 | 17 : 56 | |

passenger load in each station segment. In Scenario 4, the difference in the spatial distribution of passenger flow is not considered, and the passenger load in each station segment is calculated according to the average full-line load factor of each train. The model proposed in this paper is used to calculate the energy consumption in the four scenarios, each scenario uses PSO-GA to calculate 10 times, and the solution with the lowest net energy consumption is taken as the final optimization scheme for analysis.

One iteration of the algorithm requires 1–2 minutes, and a total of approximately 4 hours is required to obtain the complete optimization results. Figure 7 shows the variation process of the total energy consumption of the optimal individual timetable in the iteration process of scenario 1. The target value of the optimal individual exhibits a downward trend before the 134th iteration and stabilizes and reaches the optimal solution after the 134th iteration.

Table 4 compares the energy-saving effects of the four scenarios. According to Table 4, in Scenario 1, the net energy consumption of the optimized timetable is 5169.67 kW·h lower than that of the existing scheme, showing a significant energy-saving effect. The net energy consumption of the timetable in Scenario 2 is 10282.91 kW·h more than that in Scenario 1, and the total traction energy consumption and the amount of regenerative braking energy utilized are also higher than those in Scenario 1, but the two scenarios have the same utilization efficiency of regenerative braking energy. This is because the maximum traction force and braking force in the example can both meet the requirements of maximum acceleration and maximum deceleration during train operation between stations. Therefore, the energy-saving optimization strategy for the entire metro line is the same. Increase in train mass lead to increases in energy consumption and production, which again shows that changes in train mass affect the energy consumption calculation results. The net energy consumption values of the timetables in Scenario 3 and Scenario 4 are 1,673.30 kW·h and 3,301.98 kW·h higher than that in Scenario 1, respectively, and their total traction energy consumption values are 1029.32 kW·h and 1999.80 kW·h higher than that in Scenario 1, respectively, whereas their energy utilization efficiencies are 12.18% and 20.23% lower than that in Scenario 1, respectively. The results indicate that the regenerative braking energy cannot be fully utilized by considering the passenger flow distribution from the temporal or spatial perspective alone. In addition, the optimization effect of Scenario 3 is slightly better than that of Scenario 4, which indicates that the analysis of the spatial distribution pattern of passenger flow is more conducive to improving the energy-saving efficiency than considering the temporal distribution of passenger flow alone. However, the study period is only an evening peak, when most of the passengers travel for commuting purposes, with the relatively fixed OD points of companies, schools, and homes. Therefore, this result is applicable only to the periods with relatively stable OD along the whole line.

Table 5 compares the optimization schemes for the interstation running time and dwell time of Scenario 1 and Scenario 4. According to Table 5, the full-line running times of Scenario 1 in the upstream and downstream directions

Table 4: Comparison of energy-saving effects under the four Scenarios.

| Indicators/test conditions | Scenario 1 | Scenario 2 | Scenario 3 | Scenario 4 |
|---|---|---|---|---|
| Net energy consumption of the timetable/(kW·h) | 19922.97 | 30205.82 | 21596.27 | 23224.95 |
| Total traction energy consumption/(kW·h) | 25542.56 | 38725.83 | 26571.87 | 27542.36 |
| Regenerative braking energy utilization/(kW·h) | 5619.59 | 8520.02 | 4975.61 | 4317.41 |
| Regenerative braking energy utilization efficiency/% | 54.27 | 54.27 | 47.66 | 43.29 |

Table 5: Comparison of optimization schemes between Scenario 1 and Scenario 4.

| Station number | Interval running time adjustments | | Dwell time adjustment, s | | Station number | Interval running time adjustment, s | | Dwell time adjustment, s | |
|---|---|---|---|---|---|---|---|---|---|
| | Scenario 1 | Scenario 4 | Scenario 1 | Scenario 4 | | Scenario 1 | Scenario 4 | Scenario 1 | Scenario 4 |
| 1 | +5 | +5 | — | — | 44 | −4 | −4 | — | — |
| 2 | +5 | +4 | +5 | +3 | 43 | −3 | +2 | +2 | −2 |
| 3 | −2 | −1 | 0 | −2 | 42 | 0 | +4 | −2 | +5 |
| 4 | −3 | +2 | +2 | +3 | 41 | +2 | +5 | −5 | +2 |
| 5 | +2 | −1 | −5 | −5 | 40 | −5 | −1 | −5 | −4 |
| 6 | −4 | +5 | +5 | +5 | 39 | +4 | +5 | +5 | +2 |
| 7 | +3 | +1 | −5 | −5 | 38 | 0 | −2 | +5 | −1 |
| 8 | −1 | −1 | +1 | +5 | 37 | −5 | +5 | −2 | −5 |
| 9 | +5 | +1 | +4 | +4 | 36 | +5 | −4 | +4 | +1 |
| 10 | +3 | −1 | 0 | −5 | 35 | −3 | −5 | 0 | −2 |
| 11 | +2 | −2 | +5 | −2 | 34 | +5 | +5 | +5 | +4 |
| 12 | −3 | +2 | 0 | +2 | 33 | +5 | +2 | +5 | +5 |
| 13 | −5 | −5 | +5 | +5 | 32 | +5 | +5 | +5 | +5 |
| 14 | +5 | +3 | −5 | −5 | 31 | +4 | −5 | −5 | +5 |
| 15 | +2 | +2 | −3 | +4 | 30 | +4 | +1 | −1 | +5 |
| 16 | −5 | +5 | −5 | −5 | 29 | +5 | +5 | −3 | +5 |
| 17 | +5 | −1 | +5 | +5 | 28 | −1 | −3 | +5 | −5 |
| 18 | +3 | −1 | −5 | −5 | 27 | +1 | −1 | −3 | −2 |
| 19 | −2 | −3 | −1 | −3 | 26 | −1 | +5 | −1 | −5 |
| 20 | +2 | +3 | +5 | −2 | 25 | −2 | −1 | −5 | 0 |
| 21 | +3 | +3 | +5 | +5 | 24 | +4 | +4 | +5 | +5 |
| 22 | — | — | — | — | 23 | — | — | — | — |
| Total | +20 | +20 | | | | +20 | +20 | | |

each increases by 20 s after the optimization, and the interstation running time and dwell time at each station either increases or decreases. The running time of the 1st, 2nd, 9th, 14th, and 17th station segments in the upstream direction and the 29th, 32nd, 33rd, 34th, and 36th station segments in the downstream direction increase the most (by 5 s); the running time of the 13th and 16th station segments in the upstream direction and the 37th and 40th station segments in the downstream direction decrease the most (by 5 s). Although the variations in the full-line running times in the upstream and downstream directions in the optimization results under Scenario 4 are the same as those in Scenario 1, there is a certain difference in the specific time adjustment durations of each station segment and station. The train departing at 17 : 03 is used as an example for further analysis. Figure 8 shows the variation in the actual passenger load of this train over the whole line, and Figure 9 compares the power curves of this train in Scenarios 1 and 4.

Figure 8 shows that the spatial distribution of the passenger flow in the upstream direction of Qingdao Metro Line 3 during the evening rush hours exhibits the characteristics of low passenger loads in the station segments at both ends of the line and high passenger loads in the middle station segments. In Figure 9, a positive power value means that the train is in the traction mode, while a negative value means that it is in the braking mode, and positive peak values and negative peak values appear alternately. Each pair of adjacent positive and negative peaks indicates that the train passes through a station segment. Figure 9 shows that in Scenarios 1 and 4, the different turning points of the power curves indicate that there are differences in the time nodes for implementing the traction and braking modes during the full-line train operation. In addition, for the same running time, the maximum power of Scenario 4 in station segments 1 and 21 is greater than that in Scenario 1, and the maximum power of Scenario 1 in station segments 8, 13, and 15 is greater than that in Scenario 4. In example, it is assumed that the speed curve of the train in each station segment is three-stage or four-stage and that the train can run at the maximum acceleration and deceleration. Hence, only one speed curve exists for each interstation running time. As shown in Figure 8, when the passenger load in each station segment is higher than the average passenger load of the entire line, greater traction and braking forces are needed in Scenario 1 under the same running time, which results in a greater absolute power value during the

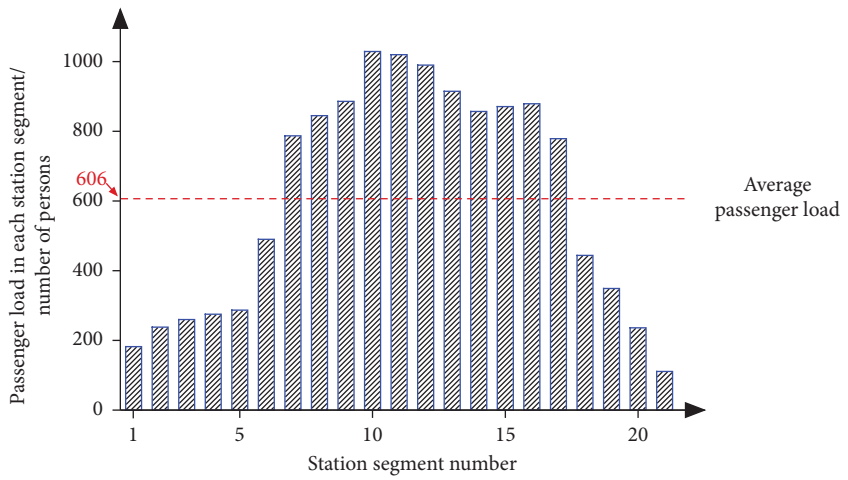


Figure 8: Passenger load in each station segment in the upstream direction at 17 : 03.

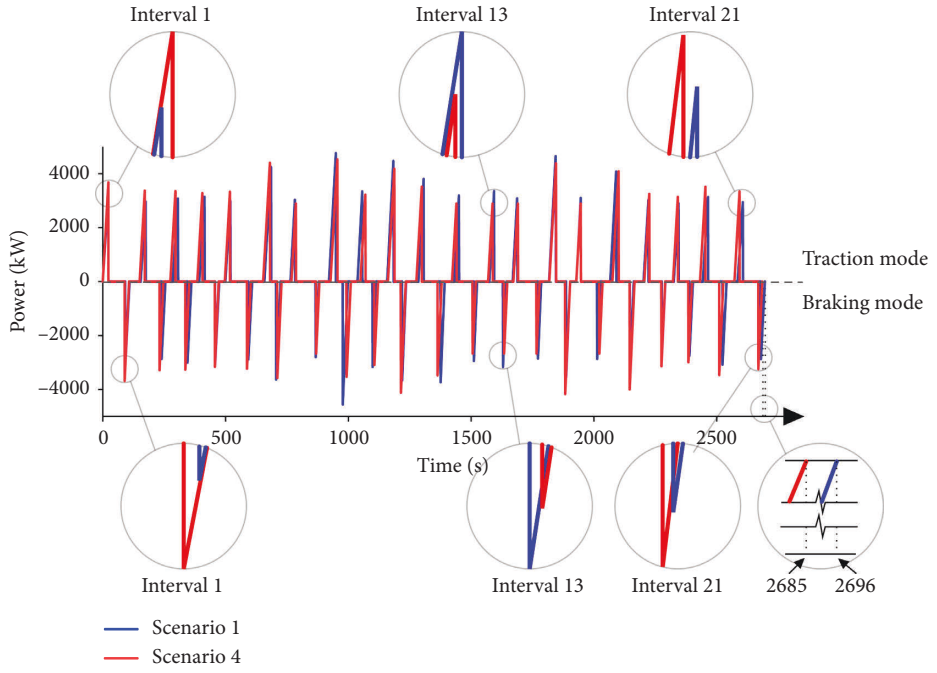


Figure 9: Comparison of the power curves of the train departing at 17 : 03 in the upstream direction in Scenario 1 and Scenario 4.

traction and braking processes. Similarly, the situation when the passenger load in each station segment is lower than the average passenger load of the whole line can be analyzed. The above results show that considering the difference in the passenger load between station segments affects the energy-saving strategy of train operation and the timetable optimization scheme to a certain extent and can improve the regenerative braking energy utilization efficiency compared with that obtained at the same constant passenger load for all station segments. In general, in the study of the energy-saving train timetable optimization problem, accurate analysis of passenger flow patterns and consideration of the difference in the dynamic distribution of passenger flow between station segments can maximize the energy-saving potential and increase the energy efficiency of the metro system. The experimental design and results in this section can provide reference for the daily operation strategy of metro corporations, further save energy consumption costs, achieve energy conservation, and emission reduction and conform to China's national policy of building an environment-friendly society.

## 6. Discussion

The pattern of cumulative passenger flow demand was fitted using the AFC data, and the OD demand time-varying matrix is established for the entire line. The calculation of passenger load in each station segment is included in the modelling of the energy-saving train timetable optimization problem. The effectiveness of the optimization method and

the necessity of considering the dynamic passenger flow distribution are verified by a case study. However, there are still some issues worth discussing in this process.

(1) The passenger flow demand is continuous and time-varying, while the timetable is discrete and stable. Therefore, effectively coupling the two has a great impact on the calculation of the speed curve and the energy consumption associated with the timetable. In this paper, it is not possible to balance the computational speed and the accuracy of the results during the model computations. When the departure frequency in the timetable increases greatly, the total computation time increases substantially. Therefore, finding an efficient and reliable solution method or further optimizing the solution architecture of the model is a direction worth further exploration.

(2) Although the changes in the passenger load in each station segment have been incorporated into the model construction, many factors have not been taken into account, such as the uncertainty of the number of boarding and alighting passengers or the passenger retention on the platform. Further consideration of these factors in future studies would make the model more practical.

(3) If the speed curve between stations is more complex (e.g., including more than one traction or coasting stage), the solution method for the speed curve in this paper is no longer applicable. In this case, it is feasible to select the speed curve between stations generated by the ATC system and to adjust the total running time of the whole line to the running time distribution of each station segment.

## 7. Conclusion

The energy-saving operation of the metro system plays an important role in reducing operating costs and protecting the environment. When the passenger flow changes, the difference in train mass between different station segments changes the energy-saving strategy. This paper considers the impact of passenger load variation on train energy consumption during the actual metro operation and aims to study the energy-saving train timetable optimization method when the temporal and spatial distributions of passenger flow vary.

(1) This study analyzes the cumulative travel demand of station segments of the metro line, uses the logistic function to fit the passenger flow pattern. The OD dynamic demand matrix of the entire line passenger flow is established to calculate the passenger load of trains in each interval, so that the dynamic distribution of passenger flow can be correlated with the optimization of energy-saving schedule.

(2) The passenger flow change, train operation process, and train timetable optimization are analyzed, the mathematical model aiming at minimizing the net energy consumption of the timetable is established. The decision variables are interstation running time and dwell time of trains, and constraints such as departure interval and full-line running time are considered. To deal with the large-scale and NP hard characteristics of the problem, a PSO-GA is designed to solve the model. The chromosome crossover and mutation operations in the GA are integrated into the PSO solution process, thus, improve the search efficiency.

(3) Taking Qingdao Metro Line 3 in China as an example, the traction energy consumption, the utilization of regenerative braking energy, and the net energy consumption under different scenarios are quantitatively analyzed, and their energy-saving potential and timetable optimization effect are compared. It is found that (1) the goodness of fit of the cumulative passenger flow demand curve is 0.997, with high reliability; (2) when the total train mass changes, the energy consumption of the train running between stations changes, which indicates that the variation in passenger load between station segments should be considered in the optimization of the energy-saving timetable. (3) The net energy consumption of the timetable of the optimized scheme in this paper is 5169.67 kW·h lower than that of the existing scheme, which proves the effectiveness of the method proposed in this paper. (4) The utilization efficiency of regenerative braking energy drops by 12.18% and 20.23%, respectively, if the temporal and spatial distribution differences are ignored. The difference in passenger load between station segments leads to changes in the maximum train power and consequently changes in the timetable optimization scheme. Considering the differences in the temporal and spatial distributions of the passenger flow would further improve the optimization potential of the energy-saving timetable.

## Data Availability

Some of the data used to support the findings of this study are included within the article. Others are restricted by the Qingdao Metro Group Co., Ltd., in order to protect metro operation privacy and security, which are available from Jingshuang Li, lyckfrank@yeah.net, for researchers who meet the criteria for access to confidential data.

## Conflicts of Interest

The authors declare that they have no conflicts of interest.

## Acknowledgments

This work was supported by the Shandong Provincial Natural Science Foundation of China (ZR2020MG021) and the Natural Science Foundation of China (62003182).

## References

[1] S. Su, X. Wang, and Y. Cao, "An energy-efficient train operation approach by integrating the metro timetabling and eco-driving," *IEEE Transactions on Intelligent Transportation Systems*, vol. 99, pp. 1–17, 2019.

[2] B. Bu, G. Qin, L. Li, and G. Li, "An energy efficient train dispatch and control integrated method in urban rail transit," *Energies*, vol. 11, no. 5, p. 1248, 2018.

[3] S. Su, T. Tang, and Y. Wang, "Evaluation of strategies to reducing traction energy consumption of metro systems using an optimal train control simulation model," *Energies*, vol. 9, no. 2, p. 105, 2016.

[4] L. D'Acierno, M. Botte, M. Gallo, and B. Montella, "Defining reserve times for metro systems: an analytical approach," *Journal of Advanced Transportation*, vol. 2018, no. 2, pp. 1–15, 2018.

[5] X. Yang, A. Chen, X. Li, B. Ning, and T. Tang, "An energy-efficient scheduling approach to improve the utilization of regenerative energy for metro systems," *Transportation Research Part C: Emerging Technologies*, vol. 57, pp. 13–29, 2015.

[6] V. A. Kleftakis and N. D. Hatziargyriou, "Optimal control of reversible substations and wayside storage devices for voltage stabilization and energy savings in metro railway networks," *IEEE Transactions on Transportation Electrification*, vol. 5, no. 2, pp. 515–523, 2019.

[7] J. Feng, Z. Ye, C. Wang, M. Xu, and S. Labi, "An integrated optimization model for energy saving in metro operations," *IEEE Transactions on Intelligent Transportation Systems*, vol. 20, no. 8, pp. 3059–3069, 2019.

[8] K. Ichikawa and K Kunihiko, "Application of optimization theory for bounded state variable problems to the operation of train," *Bulletin of Jsme*, vol. 11, no. 47, pp. 857–865, 1968.

[9] P. Milroy, "Aspects of automatic train control," *Ian Peter milroy*, 1980.

[10] B. Benjamin, I. Milroy, and P. Pudney, *Energy-efficient Operation of Long-Haul Trains*, Institution of Engineers, Australia, 1989.

[11] P. Pudney and P. Howlett, "Optimal driving strategies for a train journey with speed limits," *The Journal of the Australian Mathematical Society. Series B. Applied Mathematics*, vol. 36, no. 1, pp. 38–49, 1994.

[12] P. Howlett, "Optimal strategies for the control of a train," *Automatica*, vol. 32, no. 4, pp. 519–532, 1996.

[13] H. S. Hwang, "Control strategy for optimal compromise between trip time and energy consumption in a high-speed railway," *IEEE Transactions on Systems, Man, and Cybernetics - Part A: Systems and Humans*, vol. 28, no. 6, pp. 791–802, 1998.

[14] E. Khmelnitsky, "On an optimal control problem of train operation," *IEEE Transactions on Automatic Control*, vol. 45, no. 7, pp. 1257–1266, 2000.

[15] C. Chang and S. Sim, "Optimising train movements through coast control using genetic algorithms," *IEE Proceedings - Electric Power Applications*, vol. 144, no. 1, pp. 65–73, 1997.

[16] N. J. Weidong, N. L. Chongwei, and N. H. Fei, "A study on intelligent computation of methods of optimization operation for train," *IEEE Computer Society*, 2000.

[17] K. K. Wong and T. K. Ho, "Coast control for mass rapid transit railways with searching methods," *IEE Proceedings - Electric Power Applications*, vol. 151, no. 3, pp. 365–376, 2004.

[18] B. R. Ke, C. L. Lin, and C. C. Yang, "Optimisation of train energy-efficient operation for mass rapid transit systems," *IET Intelligent Transport Systems*, vol. 6, no. 1, pp. 58–66, 2012.

[19] Y. Huang, S. Gong, and Y. Cao, "Optimisation model of energy-efficient driving for train in urban rail transit based on particle swarm algorithm," *Journal of Traffic and Transportation Engineering*, 2016.

[20] S. Ahmadi, A. Dastfan, and M. Assili, "Improving energy-efficient train operation in urban railways: employing the variation of regenerative energy recovery rate," *IET Intelligent Transport Systems*, vol. 11, no. 6, pp. 349–357, 2017.

[21] Y. Cao, Z. C. Wang, F. Liu, P. Li, and G. Xie, "Bio-inspired speed curve optimization and sliding mode tracking control for subway trains," *IEEE Transactions on Vehicular Technology*, vol. 68, no. 7, pp. 6331–6342, 2019.

[22] K. Liu, X. Wang, and Z. Qu, "Research on multi-objective optimization and control algorithms for automatic train operation," Energies, 2019.

[23] A. Ramos, M. T. Pena, A. Fernández, and P. Cucala, "Mathematical programming approach to underground timetabling problem for maximizing time synchronization," *Dirección y Organización*, no. 35, pp. 88–95, 2008.

[24] K. M. Kim, O. Suk-Mun, and M. Han, "A mathematical approach for reducing the maximum traction energy: the case of Korean MRT trains," *Lecture Notes in Engineering and Computer Science*, vol. 2182, no. 1, 2010.

[25] B. Nag and M. N. Pal, "Optimal design of timetables to maximize schedule reliability & minimize energy consumption, rolling stock and crew deployment," *Social Science Electronic Publishing*, 2013.

[26] D. Fournier, F. Fages, and D. Mulard, "A greedy heuristic for optimizing metro regenerative energy usage," in *Proceedings of the International Conference on Railway Technology: Research*, April 2015.

[27] W. Hu, Q. Sun, and J. Lv, "Energy conversation based on the optimization of train timetable," *Urban Mass Transit*, vol. 19, no. 05, pp. 67–73, 2016.

[28] Z. Luo, X. Li, and N. Xiu, "A sparse optimization approach for energy-efficient timetabling in metro railway systems," *Journal of Advanced Transportation*, vol. 2018, pp. 1–19, 2018.

[29] C. Li, R. Wang, and D. Li, "Research on energy saving optimization of metro timetable using regenerative braking," *Control Theory & Applications*, vol. 36, no. 07, pp. 1024–1035, 2019.

[30] H. Lv, Y. Zhang, K. Huang, X. Yu, and J. Wu, "An energy-efficient timetable optimization approach in a Bi-DirectionUrban rail transit line: a mixed-integer linear programming model," *Energies*, vol. 12, no. 14, p. 2686, 2019.

[31] J. Liu, T. Li, and B. Cai, "Boundary identification for traction energy conservation capability of urban rail timetables: a case study of the beijing Batong line," vol. 13, no. 8, Energies, 2020.

[32] Y. Zhang, T. Zuo, M. Zhu, C. Huang, J. Li, and Z. Xu, "Research on multi-train energy saving optimization based on cooperative multi-objective particle swarm optimization algorithm," *International Journal of Energy Research*, vol. 45, no. 2, pp. 2644–2667, 2021.

[33] H. Gao, Y. Zhang, and J. Guo, "Two-stage optimization method of train energy-efficient operation based on dynamic programming," *Journal of Southwest Jiaotong University*, vol. 55, no. 05, pp. 946–954, 2020.

[34] D. He, S. Guo, Y. Chen, B. Liu, J. Chen, and W. Xiang, "Energy efficient metro train running time rescheduling model for fully automatic operation lines," *Journal of Transportation Engineering Part A Systems*, vol. 147, no. 7, 2021.

[35] J. Feng, X. Li, H. Liu, X. Gao, and B. Mao, "Optimizing the energy-efficient metro train timetable and control strategy in off-peak hours with uncertain passenger demands," *Energies*, vol. 10, no. 4, p. 436, 2017.

[36] W. Li, Q. Peng, C. Wen, and X. Xu, "Comprehensive optimization of a metro timetable considering passenger waiting time and energy efficiency," *IEEE Access*, vol. 7, pp. 160144–160167, 2019.

[37] Y. Gao, L. Yang, and Z. Gao, "Energy consumption and travel time analysis for metro lines with express/local mode," *Transportation Research Part D: Transport and Environment*, vol. 60, pp. 7–27, 2018.

[38] L. Kang, H. Sun, J. Wu, and Z. Gao, "Last train station-skipping, transfer-accessible and energy-efficient scheduling in subway networks," *Energy*, vol. 206, Article ID 118127, 2020.

[39] Y. Qu, H. Wang, J. Wu, X. Yang, H. Yin, and L. Zhou, "Robust optimization of train timetable and energy efficiency in urban rail transit: a two-stage approach," *Computers & Industrial Engineering*, vol. 146, Article ID 106594, 2020.

[40] H. Liu, T. Tang, and X. Xia, "A timetable optimization model to maximize regenerative energy utilization in subway systems," *Journal of Beijing Jiaotong University*, vol. 43, no. 1, pp. 71–78, 2019.

[41] D. Canca, A. Zarzo, E. Algaba, and E. Barrena, "Confrontation of Different Objectives in the determination of train scheduling," *Procedia - Social and Behavioral Sciences*, vol. 20, pp. 302–312, 2011.

[42] E. Barrena, D. Canca, L. C. Coelho, and G. Laporte, "Single-line rail rapid transit timetabling under dynamic passenger demand," *Transportation Research Part B: Methodological*, vol. 70, no. dec, pp. 134–150, 2014.

[43] S. Yang, J. Wu, and H. Sun, "Bi-objective nonlinear programming with minimum energy consumption and passenger waiting time for metro systems, based on the real-world smart-card data," *Transportation Business*, vol. 6, no. 4, pp. 1–18, 2017.

[44] Z. Gao and L. Yang, "Energy-saving operation approaches for urban rail transit systems," *Frontiers of Engineering Management*, vol. 6, no. 2, pp. 139–151, 2019.